Article

The Strength Characterisation of Concrete Made with Alumina Waste Filler

Jonathan Oti * , **John Kinuthia** and **Blessing Adeleke**

School of Engineering, Faculty of Computing, Engineering and Science, University of South Wales, Pontypridd CF37 1DL, UK; john.kinuthia@southwales.ac.uk (J.K.); blessing.adeleke@southwales.ac.uk (B.A.)
* Correspondence: Jonathan.oti@southwales.ac.uk; Tel.: +44-144-3483-452

check for updates

Abstract: This study covers an in-depth investigation into the properties and practicality of the utilization of up to 40% Alumina Waste Filler (AWF) as a partial Portland Cement (PC) replacement material. AWF is a by-product from the recycling of aluminium, produced when salt slag is smelted and cleaned. Its use in concrete will lessen the landfill requirements for AWF disposal, and reduce the strain of the growing requirements and cost of PC. The results obtained from this study showed that the addition of AWF to the concrete mix caused a reduction in the compressive and tensile splitting strength values, and a less-workable concrete was achieved for every increase in the quantity of AWF added to each mix. The addition of AWF influenced the hydration reaction process and reduced the cumulative production of the heat of hydration over time, whilst the permeability of the concrete decreased.

Keywords: sustainable concrete; industrial by-products; durability; mechanical strength; permeability; isothermal calorimetry

1. Introduction

Concrete is the most widely-used construction material in the world due to its flexibility and ability to be moulded into different shapes. It is an engineering material that binds particles together, simulating the compact properties of rock. Concrete is made of a coarse and fine aggregate, bound together through a hydraulic binder (Portland Cement-PC) activated by water [1]. Despite being a fantastic building material, there have been some sustainability concerns with concrete, especially in relation to its main component (PC). Zongjin [2] attributed this concern as the intensive energy requirements of PC production, with an approximate 1 tonne of carbon dioxide (CO_2) released into the environment. This has led to the use of several industrial and construction wastes, such as Pulverised Fuel Ash (PFA), Ground Granulated Blastfurnace Slag (GGBS), Brick Dust Waste (BDW) and Silica Fume (SF), which have significant benefits for the workability and strength properties of concrete. This has helped to push forward the use of industrial wastes in specific replacements in order to mitigate the environmental damage caused by the dumping of industrial waste and by-products into landfills, and the production and use of PC.

According to the World Business Council for Sustainable Development, approximately 5–7% of man-made global CO_2 emissions come from the production of Portland cement. The production of cement is set to continue increasing as the demand worldwide is continuing to increase, especially where emerging economies need cement for housing and infrastructure [3]. Miqueleiz et al. [4] demonstrated the potential use of AWF in the production of building materials (unfired bricks) as a partial replacement for clay, and recommended its use based on its added environmental benefits. Gritsada and Natt [5] also utilised AWF as a replacement for fine aggregate in the production of self-consolidating concrete. The results demonstrated that AWF incorporating between 25–75% of the fine aggregate produced

some mechanical benefits that were significant enough to include its practicality in self-consolidating concrete. The permeability of concrete is one of the most important factors when considering its durability index, which will be of interest to engineers when specifying their choice of concrete grade for a project. Hamakareem [6] defined concrete permeability as the property associated with the rate of flow of fluids through a porous material. This infiltration of harmful materials can affect the durability of the concrete. Furthermore, if the concrete was to become saturated with water due to poor permeability, it would be more vulnerable to frost action.

The performance of cementitious formulations has recently become a key focal point of interest with respect to the monitoring of heat evolution during a hydration process. This stems from the hypothesis that the performance of cementitious systems could be predicted by monitoring the heat generated during hydration, which can be measured by a calorimeter [7]. Therefore, the heat of hydration (HOH), which is the integral of the heat production rate (thermal power) in a hydration process, is very essential when investigating hydration rates, the variation in the temperature changes within the cementitious binder composition, and the classification of binder compositions based on their reactivity [8,9]. Some calorimetric investigations have been used to evaluate the hydration kinetics of Portland cement [7,10,11]. Nevertheless, the application of calorimetric analysis for industrial waste formulations such as AWF has not been established in the existing literature. Therefore, the calorimetric test will be employed in order to further simplify the expected complexity of the hydration reaction of the emerging AWF binder system into a simpler analytic form that can be understood.

Previously, in Europe, the aluminium salt slag which was produced was stored in landfills. However, under the increased regulation which resulted from the identified environmental concerns, AWF was created for reuse by the reutilisation of the produced aluminium salt slag [12]. This research covers a detailed investigation into the engineering properties of concrete manufactured using AWF as a partial replacement for PC, in an effort to reduce the demand for PC. This will ultimately reduce the carbon footprint associated with the material, and produce an understanding of the hydration reaction of the developed binders using isothermal calorimetry. Various concrete mixtures were developed using varying percentages of AF waste as a cement replacement, with 100% Portland cement as a control.

2. Materials and Methods

2.1. Materials

The materials used in this investigation are Portland cement (PC), Alumina Waste Filler (AWF), limestone (coarse aggregate), sand (fine aggregate) and deionized water. The PC was manufactured according to BS EN 197-1 [13], and was supplied by Lafarge Cement UK.

AWF is an industrial waste product from aluminium recycling; about 110,000 tonnes per year is generated as secondary waste during the valorisation process of aluminium salt slag [4], and it was supplied by Befesa Salt Slags Limited, UK. AWF was developed by melting the scrap aluminium in a rotary furnace underneath a bath of molten salt, which floats on the surface of the aluminium and minimises the loss of oxides in the aluminium. Small amounts of aluminium oxide become trapped in the molten salt whilst the molten aluminium is tapped out. Once the molten salt solidifies, salt slag is produced. This salt slag is a hazardous waste which needs to be disposed of in a controlled manner or recycled in a more efficient and environmentally sustainable manner, such as the manner used in the research. Some of the oxide composition and physical properties of PC and AWF, respectively, are shown in Table 1.

Table 1. Some of the oxide composition and physical properties of AWF and PC.

Oxide	PC (%)	AFW (%)
CaO	63.00	1
SiO_2	20.00	8
Al_2O_3	6.00	70
MgO	4.21	6
Fe_2O_3	3.00	–
MnO	0.03–1.11	–
S^{2-}	–	–
SO_3	2.30	–
SO_4	–	–
K_2O	–	–
N_2O	–	–
CO_3	–	–
Soluble Silica	–	–
Properties		
Insoluble Residue	0.5	–
Bulk Density (kg/m^3)	1400	1200
Relative Density	3.1	–
Blaine fineness (m^2/kg)	365	–
pH	12.86	–
Colour	Grey	Grey
Glass Content	–	–

PC = Portland cement; AWF = Alumina Waste Filler.

The limestone sizes (coarse aggregate) used throughout this investigation were 10 mm and 20 mm, while the sand (fine aggregate) was a natural sea-dredged sand from the Bristol Channel. The aggregates were supplied by a local quarry, and were complied with the requirements of BS EN 12620:2002 +A1 [14]. Table 2 shows some of the geometrical, mechanical and physical properties of the limestone aggregate (coarse aggregate) and sand (fine aggregate), in compliance with BS EN 1097-6 [15], BS EN 933-4 [16] and BS 812–112 [17].

Table 2. The geometrical, mechanical and physical properties of the aggregates.

Property	Sand	Limestone Aggregates	
		(10 mm)	(20 mm)
Water absorption (%)	0.85	1.5	1.1
Saturated density (Mg/m^3)	2.82	2.68	2.65
Dry density (Mg/m^3)	2.71	2.57	2.54
Shape index (%)	–	12	7
Impact value (%)	–	23	15

2.2. Mix Design and Sample Preparation

The control mix (100PC-0AWF) for the concrete used in this research was a binder:sand:aggregate proportion of 1:2.5:3.5, using a water/binder ratio of 0.65. Based on the control mix for the concrete, the investigation used up to 40% AWF to replace some of the Portland Cement (PC) in the control mix in various combinations, as shown in Table 3. The purpose was to obtain a cost-effective and useable concrete. Dry sample mixtures for the binders were developed for each of the mix compositions (90PC-10AWF; 80PC-20AWF; 70PC-30AWF and 60PC-40AWF), and were thoroughly mixed together in a mechanical mixer for 10 mins in order to ensure homogeneity for the analytical investigation (Isothermal Calorimetry).

Table 3. The mix combination for all of the concrete mixes.

Composition	PC (Kg/m^3)	AFW (kg/)	Limestone Aggregate (kg/m^3)		Sand (kg/m^3)	Water (kg/m^3)
			10 mm	20 mm		
100PC-0AWF (Control)	314	0	549	549	784	204
90PC-10AWF	282.6	31.4	549	549	784	204
80PC-20AWF	251.2	62.8	549	549	784	204
70PC-30AWF	219.8	94.2	549	549	784	204
60PC-40AWF	188.4	125.6	549	549	784	204

PC = Portland cement; AWF = Alumina Waste Filler.

Cube (100 mm × 100 mm × 100 mm) and cylinder test samples (100 mm diameter × 200 mm) specimens were used in the production of all of the concrete. For all of the mix compositions, the test specimens were prepared in accordance with BS EN 206 [18], BS EN 12350-1 [19] and BS EN 12390-1 [20]. The consistency of the fresh concrete was measured using a slump test in accordance with BS EN 12350-2 [21], and a compaction index test in compliance with BS EN 12350-4 [22]. The de-moulding of the test specimens was carried out after 24 h. The curing of the test specimens was carried out in accordance with BS EN 12390-2 [23]. All of the cube specimens were tested for their 7, 28, and 90 day compressive strength in accordance with BS EN 12390-3 [24], and for their tensile splitting strength for 28 days, in compliance with BS EN 12390-6 [25]. The results reported are the average obtained from three individual test specimens for both compressive and tensile splitting strength values.

2.3. Calorimetric Analysis

A calorimetric analysis was carried out to investigate the hydration kinetics and reactivity levels of the designed mix blends by directly measuring the rate of heat produced during the hydration process within a thermostated Isothermal calorimetry chamber. The heat production rate (thermal power) was determined at a controlled temperature (25 °C) for a period of 72 h using a Toni-CAL Isothermal Calorimeter from Toni Technik, Germany. In total, 5 g of the dry sample mixtures for the different mixes were placed in the calorimetric chamber in a specimen tube [26]. The heat produced during the hydration reaction was detected, stored and analysed using a data acquisition system (Toni-DCA Analysis software) according to BS EN 196-11 [27].

2.4. Water Permeability Test

The water permeability test was undertaken after a period of 28 days of curing for each of the mixes, and the test was carried out in accordance with BS EN 12390-8 [28]. Concrete cubes were fastened into the concrete water permeability apparatus with the appropriate bolts, followed by bolts to secure a cover over the cube and chamber. A pre-test inspection was necessary in order to ensure that all of the seals were in full working order, and all of the bolts were fastened securely. Once the testing began, the samples were gradually subjected to pressures of up to 30 Bar. As water passed through the concrete, it was collected beneath the apparatus in a measuring cylinder, whilst time to collect the amount of water was monitored. The pressure, the quantity of water and the time necessary were recorded in order to ensure the mathematical calculation of the water permeability for each concrete mix.

3. Results and Discussion

3.1. Consistency of Concrete

The consistency results for the developed concrete mixes in terms of their slump values is shown in Figure 1. The control mix attained the highest slump value of 69 mm, while the lowest slump (20 mm) was experienced by mix 60 PC-40AWF. Close observation also shows a gradual reduction in the slump values (40 mm, 35 mm, 25 mm, 20 mm) for all the mixes with every percentage replacement

increase of AWF with PC respectively. This shows that the more AWF contained within each mix, the lower the slump value. This suggests that increased levels of AWF could produce drier mixes and reduce workability.
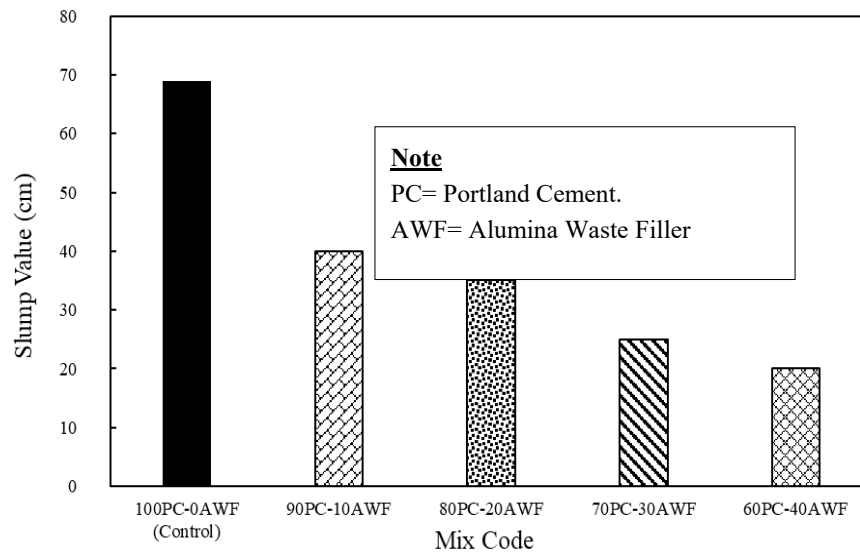

Figure 1. Slump values for the concrete mixes.

Figure 2 shows the results of the compaction index obtained for each of the investigated mixes (90PC-10AWF; 80PC-20AWF; 70PC-30AWF; and 60PC-40AWF), which gives an indication to the workability of the fresh state of concrete. The compaction index obtained for the developed mixes was within the range of 1.18 to 1.29, with mix 60PC-40AWF attaining the highest compaction index value of 1.29, while the lowest value (1.18) was attained by the control mix. A gradual increase in the compaction index values was also attained for every percentage increase in replacement levels of AWF with PC, respectively. This shows that increased amounts of AWF within the mix result in higher compaction index values. This also suggests that the more AWF is contained within the mix, the less workable it becomes.
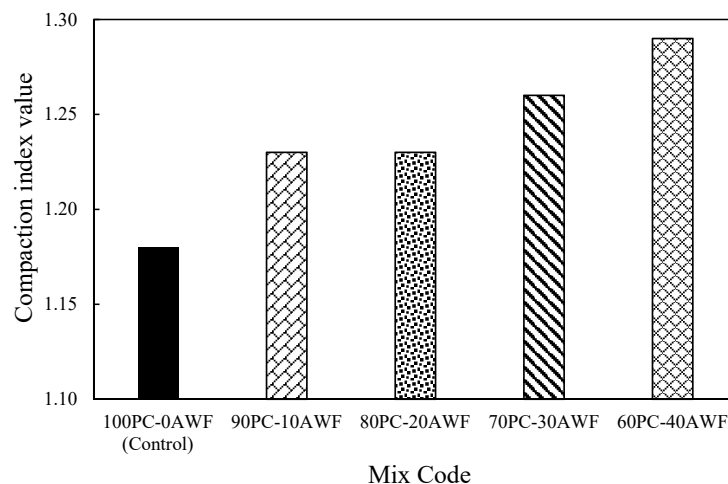

Figure 2. Compaction index values for the concrete mixes.

Generally, the slump and compaction index results indicate that the control mix is an S2 Standard mix (slump values between 50 mm and 90 mm), while the other mixes was classed as an S1 Dry Mixes (slump values between 10 and 40 mm) in accordance with BS EN 12350-2 [21]. Since the target slump for S1 and S2 mixes is 20 mm and 70 mm, respectively [21], an S2 mix can experience a change in its

slump classification to S1 by the application of 40% replacement of PC with AWF. This suggests that, if a mix requires a reduction in slump classification, the introduction of AWF into the mix should dry it. The observed dryness of the mixes for increased levels of AWF with PC is in line with the works carried out by Gritsada and Natt [5] on the use of AWF as a fine aggregate replacement, which suggested that AWF influences the consistency (slump values) of any developed mix. However, the reduced workability of the mixes containing AF waste can be useful in certain civil engineering applications. Concrete2you [29] suggested that concrete classed as S1 can be utilised in situations where a dry mix is preferred for certain civil engineering applications such as kerb and pipework, as well as other lean concrete for beddings and mass filling applications. This can be a likely use for the incorporation of AWF in concrete in order to reduce the use of PC. A possible solution to the reduced workability in the application of AWF as a partial replacement of PC could be to increase the water:cement ratio, along with the reduction of the compression resistance. However, care must be taken in this regard, as any ambiguous increase in the water content could result in the concrete bleeding.

3.2. Strength Test of Hardened Concrete

The results obtained from the compressive strength test for all of the investigated concrete mixes at 7, 28, and 90 days into the curing period can be seen in Figure 3. The control mix produced the highest compressive strength value of 37.2 N/mm^2, while mix 60 PC-40AWF achieved a compressive strength of 25.7 N/mm^2 after a 90 day curing period. A similar trend of compressive strength reduction occurred for all of the concrete mixes at 7 and 28 days. This shows a constant trend of decreasing compressive strength values for every increase in the percentage of the replacement of AWF with PC.
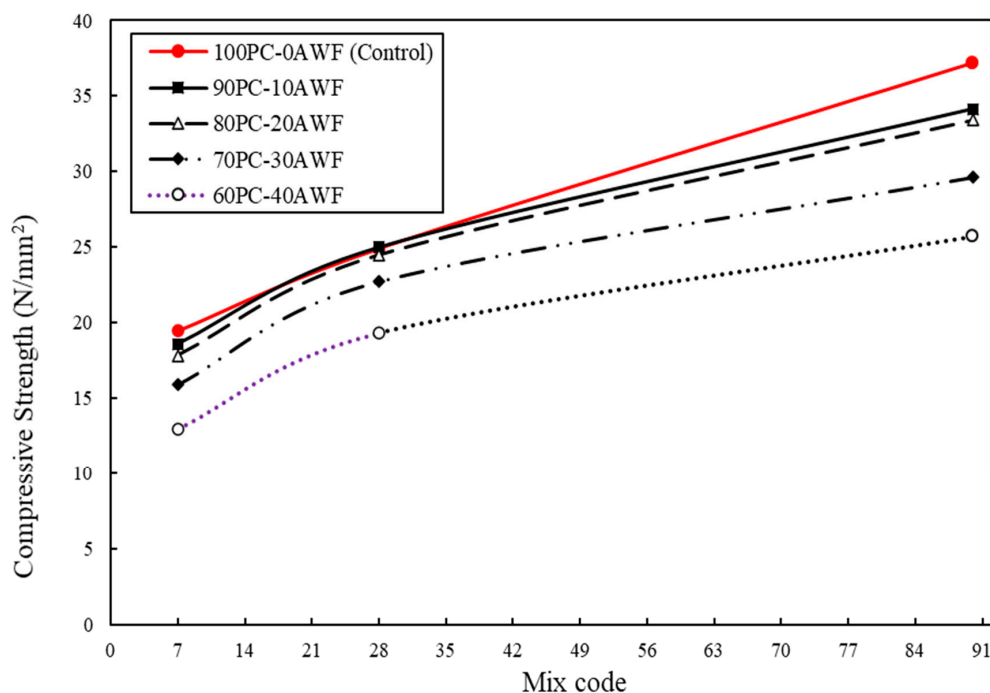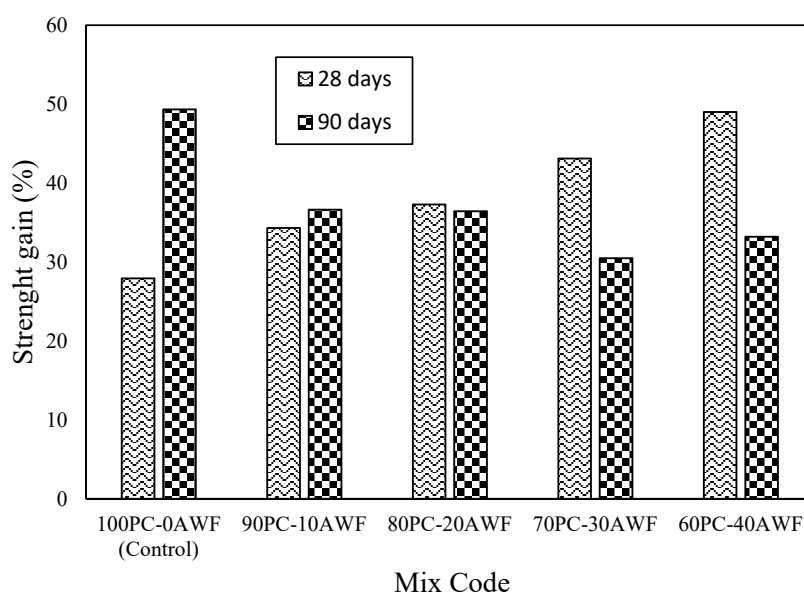

Figure 3. Compressive strength development for the concrete mixes.

A gradual increase in compressive strength values can be observed for all of the concrete mixes over 90 days. This was more pronounced for the control mix, where it showed a linear curve (see Figure 3) with a 28% and 49% strength gain at 28 and 90 days, respectively.

Despite the gradual increase in the compressive strength gain for all of the investigated mixes, the control mix attained a higher strength compared with all of the other mixes (see Figure 4). This trend was also similar after a 90 day curing period, where there was a gradual reduction in the strength gain for every percentage replacement of AWF with PC (see Figure 4). This suggests that the increase of

AWF in a concrete mix produces a reduction in its compressive strength across all curing ages (7, 28, and 90 days).

Figure 4. Compressive strength gain (%) development for the concrete mixes at 28 and 90 days.

Figure 5 shows the tensile splitting strength test results at 28 days for the investigated hardened concrete mixes. The control mix produced the highest tensile splitting strength value of 3.3 N/mm^2, while mix B4 (70%PC:30%AFW) produced the lowest tensile splitting strength value of 2.8 N/mm^2.
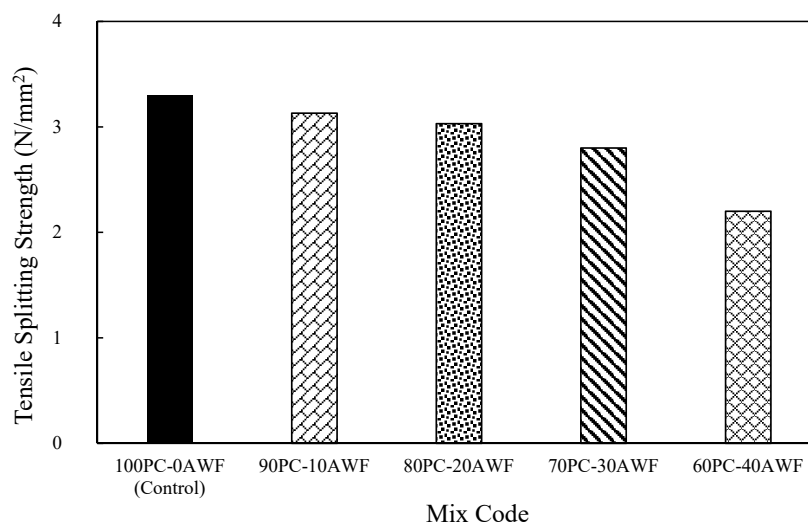
**Figure 5.** Tensile strength development for the concrete mixes.

A gradual reduction in the tensile splitting strength values were also evident for every percentage replacement of AWF with PC (Figure 5). This was very pronounced for mix 60 PC:40AWF, which failed during the demoulding process. This result suggests that any increase in AWF content within a concrete mix will cause a decrease in tensile splitting strength. Although a tensile splitting test is not very needed in un-reinforced concrete (since concrete performs better in compression), it is important to carry the test out for research completeness.

The identified reduction in both the compressive and tensile strength values could be due to the lower levels of Ca present within each mix composition (varying the percentage replacement of PC with AWF) to produce C–S–H gel during the hydration reaction, which is responsible for strength

gain [30,31]. This could also be attributed to the presence of air voids within the concrete due to insufficient compaction during the preparation of the fresh concrete. Since the concretes produced from mixes 100PC-0AWF, 90PC-10AWF, 80PC-20AWF and 70PC-30AWF were able to achieve a minimum compressive strength of 25 N/mm^2 at 28 days, they can be classified as concretes that are suitable for certain structural applications such as house slabs, driveways, footings and footpaths, which need little emphasis on high strength [26].

3.3. Water Permeability Test of Hardened Concrete

Figure 6 and Table 4 show the results for the water permeability test for the produced hardened concrete for all of the investigated concrete mixes (100PC-0AWF, 90PC-10AWF, 80PC-20AWF, 70PC-30AWF and 60PC-40AWF). There were some observed variations in the water permeability for the varying concrete mixes with the addition of AWF. Mix 80PC-20AWF experienced the highest level of water permeability, while mix 60PC-40AWF produced the lowest level of water permeability. The observation showed a constant trend of increasing water permeability for every percentage increase in the amount of AWF replaced with PC, except in for mix 60PC-40AWF. Despite this anomaly, it can still be seen that the more AWF is contained within the mix, the less permeable the concrete becomes. This suggests that high levels of AWF reduce the water permeability of the concrete. The variation in some of the results for permeability may be due to operator skills and inaccuracies in the moulds.
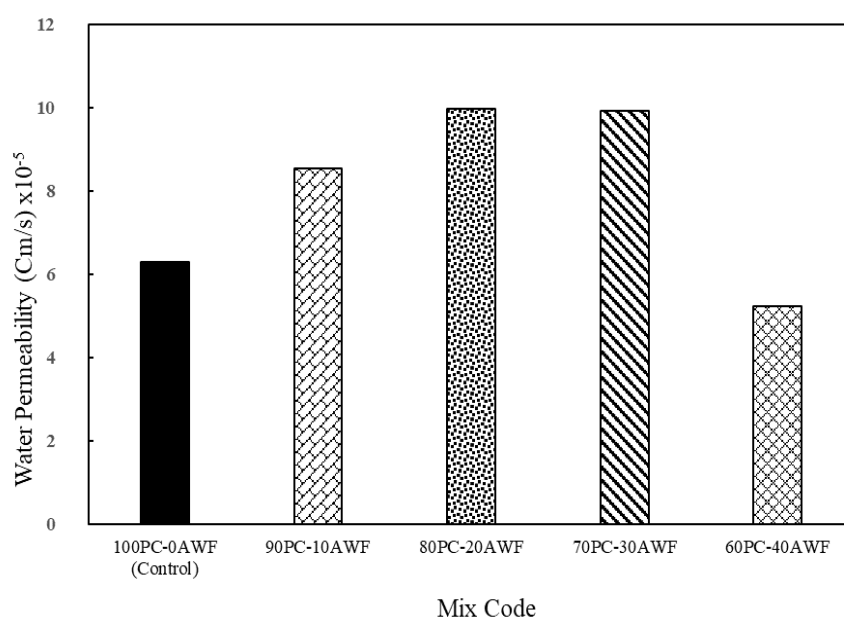
Figure 6. Water permeability for all of the concrete mixes.

Table 4. Permeability coefficients for all of the mixes.

Composition	Coefficient of Permeability (cm/s)
100PC-0AWF (Control)	6.29×10^{-5}
90PC-10AWF	8.55×10^{-5}
80PC-20AWF	9.97×10^{-5}
70PC-30AWF	9.92×10^{-5}
60PC-40AWF	5.24×10^{-5}

The reduction in water permeability may be due to the lower amounts Calcium Silicate Hydrate that is present during the hydration process. With a lower cement content, lower calcium silicate hydrate would be present, which would provide a less dense material and therefore a higher permeability.

This links the strengths, heat of hydration and permeability of the mixes to the total Calcium Silicate Hydrate present within the concrete.

Hamakareem [6] described water permeability as being dependent on three factors, such as water cement ratio, and the compaction and curing of the concrete. These identified factors could also be suggested as reasons for the variation in the water permeability of the developed mixes. Tarun et al. [32] suggested that PFA reduces the water permeability of the concrete. This is quite the opposite of the results found in this study, where the by-product (AWF) blends increased the concrete's water permeability. This could be due to the reduction in the number of fine particulates present within the Alumina Waste Filler, which makes the concrete denser and more compact.

3.4. Calorimetric Analysis of the Binders

Figure 7 shows the curve for the thermal power produced during the hydration reaction for all of the investigated mix binders. Two exothermic thermal power peaks were identified over the observatory period. The first peak was observed immediately after the commencement of the hydration reaction (initial reaction stage), while the second exothermic thermal power peak appeared at a much later stage (after the induction stage).
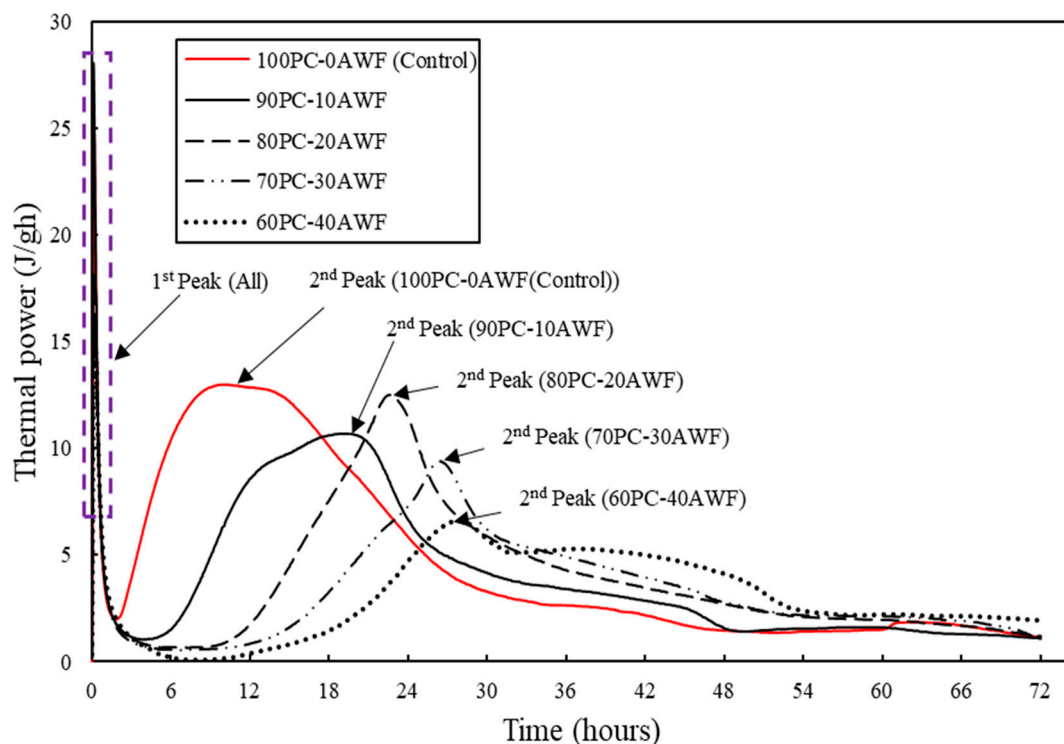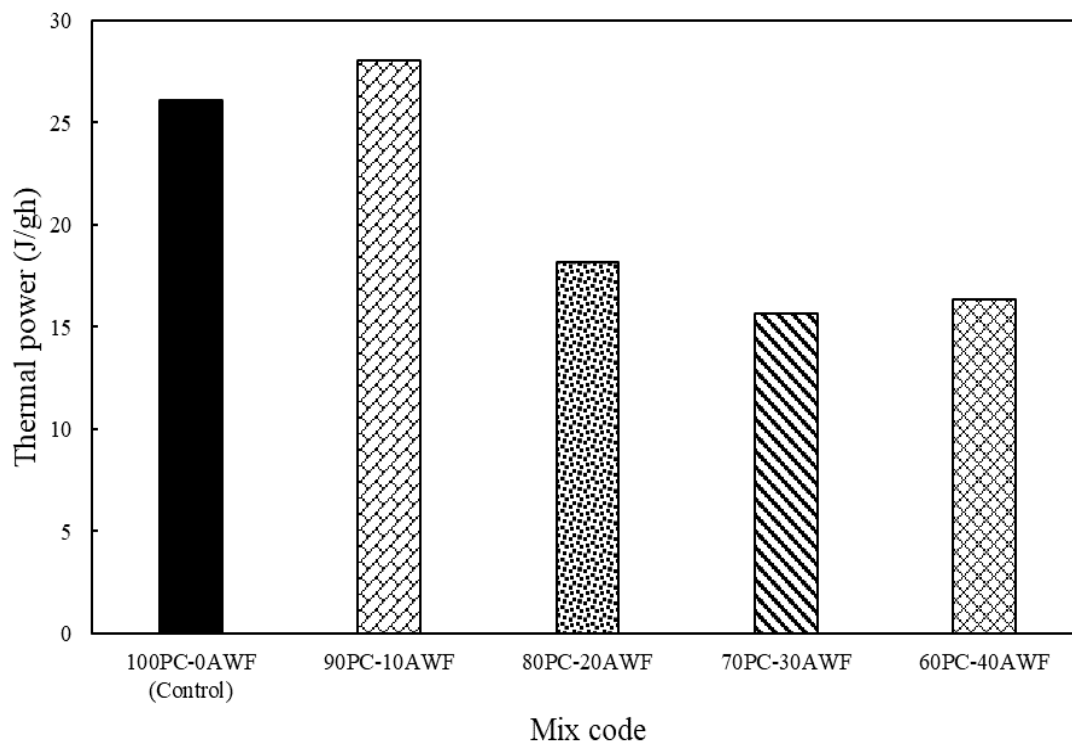

Figure 7. Calorimetric thermal power production for all of the mixes.

The first exothermic thermal peaks are further illustrated in Figure 8. The largest amount of heat production during the hydration reaction was observed for mix 90PC-10AWF, while mix 70PC-30AWF produced the lowest thermal power. The very rapid increase in thermal production at the initial reaction stages for all of the binders (first peak) can be attributed to the combined exothermic reaction experienced during the hydration of calcium oxide present within the binder mix compositions. Bensted [33] and Pang et al. [34] also attributed this peak generation to the formation of a crystalline compound commonly known as ettringite, resulting from the hydration reaction that occurs during the complete decomposition of gypsum that may be present within binders from the transformation of calcium sulphate hemihydrate ($CaSO_4 \cdot 1/2H_2O$) to calcium sulphate dihydrate ($CaSO_4 \cdot 2H_2O$).

Figure 8. First calorimetric thermal power for all of the mixes.

The control mix obtained the highest second exothermic thermal peak of 13 J/gh (Figure 7), while there was a gradual reduction in the heat production (10.7 J/gh, 9.4 J/gh and 6.6 J/gh,) for every increase in the amount of AWF in mixes 90PC-10AWF, 70PC-30AWF, and 60PC-40AWF, respectively. However, an anomaly occurred with an increased amount of heat production (12.5 J/gh) for mix 80PC-20AWF compared with 90PC-10AWF. The experienced reduction in thermal power could be as a result of the reduction in PC (calcium content) present within each mix, which necessarily requires Ca for the continuation of the hydration process, because part of the Ca within each mix has been used in the initial reaction stage (first exothermic thermal peak).

Figure 9 shows the duration for the complete production of the second exothermic peak. This reveals a gradual increase in the time and intensity of the produced exothermic peaks for the control (9.43 h), 90PC-10AWF (18.50 h), 80PC-20AWF (22.31 h), 70PC-30AWF (26.25 h) and 60PC-40AWF (27.29 h) mixes, respectively. This clearly indicates that the Ca content within a mix composition has an effect on the dissipation of its thermal power. Thomas et al. [35] attributed the duration for this second exothermic peak production as the induction period, which requires the destruction of a protective layer formed around the tricalcium silicate during this stage.

The results for the produced Heat of Hydration (HOH) for each of the mixes are presented in Figure 10. The highest HOH dissipated over the observation period (72 h) was 380 J/gh for the control mix, whilst a gradual reduction in the production of the HOH was experienced for every percentage increase in the AWF content for each investigated mix (283.7 J/gh, 276 J/gh, 239 J/gh and 225 J/gh, respectively). This suggests that more AWF within the mix reduces the total heat produced and the maximum temperature during the hydration process, whilst increasing the dormant stage. This trend is constant throughout the varying mixes. The decrease in the cumulative heat could also be due to the lower amounts of Ca present within the mix compositions with every increase in AWF, which results in the reduced formation of C–S–H (Calcium Silicate Hydrate) gel during the hydration reaction and the time taken to form the second endothermic peak. This is in line with works carried out by Snelson et al. [36], who blended PFA with PC, and suggested that the partial replacement of PC with

cementitious materials (by-product) will ultimately reduce the cumulative HOH given off during the hydration reaction process.
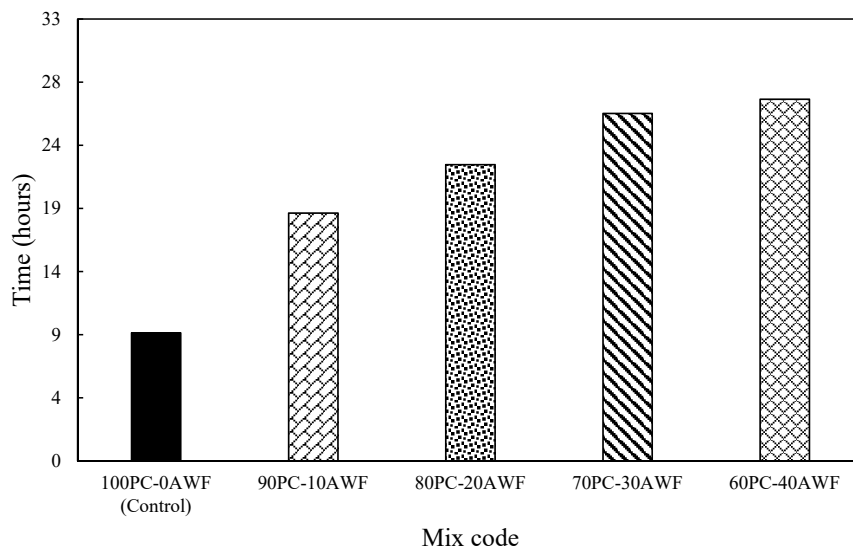
Figure 9. Time taken to produce the second calorimetric peak for all of the mixes.
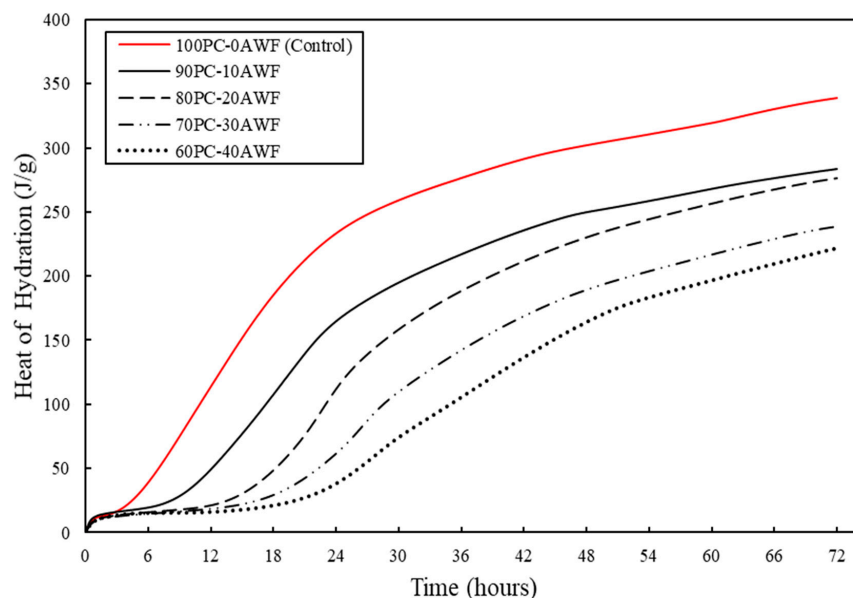
Figure 10. Calorimetric heat of hydration for all of the mixes.

4. Conclusions

From this investigation, conclusions are able to be drawn based on the investigated potentials of the utilization of Alumina Waste Filler (AWF) as a partial replacement for PC within a concrete mix. The main conclusions that can be drawn from this study are detailed below:

(1) There was variation in the slump and compaction index values observed for the concrete mixes with the further replacement of PC with AWF, which suggests that increased levels of AWF produce drier mixes and reduce workability. A possible solution to the reduced workability issues with the addition of AWF could be to increase the water:cement ratio.

(2) The reduction in both compressive and tensile strength for every percentage increase in AWF content could be due to the lower levels of Ca present within each mix composition with the

varying percentage replacement of PC with AWF to produce C–S–H gel during the hydration reaction, which is responsible for strength gain. The percentage of the reduction in the compressive strength depending on the AWF increase. Since the concrete produced from mixes 100PC-0AWF, 90PC-10AWF, 80PC-20AWF, and 70PC-30AWF were able to achieve a minimum compressive strength of 25 N/mm^2 at 28 days, they can be classified as concretes that are suitable for certain structural applications, such as house slabs, driveways, footings, and footpaths, which require little emphasis on high strength.

(3) The results obtained from the water permeability test indicate that high levels (40% and above) of AWF reduce the water permeability of the concrete and also influence the overall dark colour of the concrete mix.

(4) The results obtained from the calorimetric heat of hydration (HOH) and the rate of the heat evolution showed that the highest cumulative heat was obtained by the control, while the lowest cumulative heat was obtained from the mix where 40% of the PC used in the control mix was replaced with AWF. Little dose AWF replacements may be utilised to reduce the heat of hydration (during the reduction of the flash setting) without necessarily influencing the compressive strength negatively.

(5) Construction cost and technical barriers, such as insufficient durability data and differentiation for different applications, still hinder the global promotion of concrete utilizing high amounts of industrial by-product additives. The utilisation of up to 40% AWF to replace PC will reduce the cost of concrete production and reduce the carbon footprint of the concrete; however, the utilization of such high amounts of AWF additives whilst, at the same time, producing a workable concrete may result in workability and durability issues. Work is currently ongoing on the durability of concrete made with AWF, with increased water:cement ratios and the Life Cycle Assessment of the final product. The outcome of these possibilities will be reported in another paper.

References

1. Concrete Society. What is Concrete? 2017. Available online: http://www.concrete.org.uk/fingertips-nuggets. asp?cmd=display (accessed on 14 June 2017).

2. Zongjin, L. *Advanced Concrete Technology*, 1st ed.; John Wiley & Sons: Hoboken, NJ, USA, 2011.

3. World Business Council for Sustainable Development (WBCSD). *World Business Council for Sustainable Development: CO$_2$ and Climate Protection*; WBCSD: Geneva, Switzerland, 2015.

4. Miqueleiz, L.; Ramirez, F.; Oti, J.E.; Seco, A.; Kinthuia, J.M. Alumina filler waste as clay replacement material for unfired brick production. *Eng. Geol.* **2013**, *163*, 68–74. [CrossRef]

5. Gritsada, S.; Natt, M. Incorporation of high-volume fly ash waste and high-volume recycled alumina waste in the production of self-consolidating concrete. *J. Clean. Prod.* **2017**, *159*, 194–206.

6. Hamakareem, M.I. Permeability of Concrete and Factors Influencing It. 2019. Available online: https://theconstructor.org/concrete/permeability-concrete/1769/ (accessed on 23 May 2019).

7. Hu, J.; Ge, Z.; Wang, K. Influence of cement fineness and water-to-cement ratio on mortar early-age heat of hydration and set times. *Constr. Build. Mater.* **2014**, *50*, 657–663. [CrossRef]

8. Sedaghat, A.; Zayed, A.; Sandberg, P. Measurement and Prediction of Heat of Hydration of Portland Cement Using Isothermal Conduction Calorimetry. *J. Test. Eval.* **2013**, *41*, 943–950. [CrossRef]

9. Scrivener, K.; Snellings, R.; Lothenbach, B. *A Practical Guide to Microstructural Analysis of Cementitious Materials*; Taylor & Francis Group: Abingdon, UK, 2016.

10. Mostafa, N.Y.; Brown, P.W. Heat of hydration of high reactive pozzolans in blended cements: Isothermal conduction calorimetry. *Thermochim. Acta* **2005**, *435*, 162–167. [CrossRef]

11. Schöler, A.; Lothenbach, B.; Winnefeld, F.; Haha, M.B.; Zajac, M.; Ludwig, H.-M. Early hydration of SCM-blended Portland cements: A pore solution and isothermal calorimetry study. *Cem. Concr. Res.* **2017**, *93*, 71–82. [CrossRef]

12. Rva. Origins of Aluminium Salt Slag. 2012. Available online: http://www.rva-recycling.com/?page_id=98 (accessed on 1 April 2019).

13. British Standards Institution. *BS EN 197-1:2011—Cement. Part 1: Composition, Specifications and Conformity Criteria for Common Cements*; British Standards Institution: London, UK, 2011.

14. British Standards Institution. *BS EN 12620:2002+A1:2008—Aggregates for Concrete*; British Standards Institution: London, UK, 2008.

15. British Standards Institution. *BS EN 1097-6:2013—Tests for Mechanical and Physical Properties of Aggregates. Part 6: Determination of Particle Density and Water Absorption*; British Standards Institution: London, UK, 2013.

16. British Standards Institution. *BS EN 933-4:2008—Tests for Geometrical Properties of Aggregates. Part 4: Determination of Particle Shape—Shape Index*; British Standards Institution: London, UK, 2008.

17. British Standards Institution. *BS 812-112: 1990—Testing Aggregates. Part 112: Method for Determination of Aggregate Impact Value (AIV)*; British Standards Institution: London, UK, 1990.

18. British Standards Institution. *BS EN 206:2013+A1:2016—Concrete in Specification, Performance, Production and Conformity*; British Standards Institution: London, UK, 2013.

19. British Standards Institution. *BS EN 12350-1:2019—Testing Fresh Concrete. Part 1: Sampling and Common Apparatus*; British Standards Institution: London, UK, 2019.

20. British Standards Institution. *BS EN 12390-1:2012—Testing Hardened Concrete. Part 1: Shape, Dimensions and Other Requirements for Specimens and Moulds*; British Standards Institution: London, UK, 2012.

21. British Standards Institution. *BS EN 12350-2:2019—Testing Fresh Concrete. Part 2: Slump Test*; British Standards Institution: London, UK, 2019.

22. British Standards Institution. *BS EN 12350-4:2019—Testing Fresh Concrete. Part 4: Degree of Compactability*; British Standards Institution: London, UK, 2019.

23. British Standards Institution. *BS EN 12390-2:2019—Testing Hardened Concrete. Part 2: Making and Curing Specimens for Strength Tests*; British Standards Institution: London, UK, 2019.

24. British Standards Institution. *BS EN 12390-3:2019—Testing Hardened Concrete. Part 3: Compressive Strength of Test Specimens*; British Standards Institution: London, UK, 2019.

25. British Standards Institution. *BS EN 12390-6:2009—Testing Hardened Concrete. Part 6: Tensile Splitting Strength of Test Specimens*; British Standards Institution: London, UK, 2009.

26. British Standards Institution. *BS EN 196-7:2007—Methods of Testing Cement. Part 7: Methods of Taking and Preparing Samples of Cement*; British Standards Institution: London, UK, 2007.

27. British Standards Institution. *BS EN 196-11:2018—Methods of Testing Cement. Part 11: Heat of Hydration—Isothermal Conduction Calorimetry Method*; British Standards Institution: London, UK, 2018.

28. British Standards Institution. *BS EN 12390-8:2019. Testing Hardened Concrete. Depth of Penetration of Water under Pressure*; British Standards Institution: London, UK, 2019.

29. Concrete2you. Concrete Workability. 2007. Available online: https://www.concrete2you.com/advice/concrete-workability/ (accessed on 11 April 2007).

30. Walker, C.S.; Sutou, S.; Oda, C.; Mihara, M.; Honda, A. Calcium silicate hydrate (C–S–H) gel solubility data and a discrete solid phase model at 25 °C based on two binary non-ideal solid solutions. *Cem. Concr. Res.* **2016**, *79*, 1–30. [CrossRef]

31. Oti, J.; Kinuthia, J.; Adeleke, B.; Billong, N. Durability of Concrete Containing PFA-GGBS By-products. *J. Civ. Eng. Constr.* **2020**, *9*, 165–174. [CrossRef]

32. Tarun, R.; Naik, S.; Singh, S.; Hossain, M.M. Permeability of concrete containing large amounts of fly ash. *Cem. Concr. Res.* **1994**, *24*, 913–922.

33. Bensted, J. *Seventh International Congress on the Chemistry of Cement*; Editions Septima: Paris, France, 1980; Volume 2, Part II; pp. 1–6.

34. Pang, X.; Bentz, D.P.; Meyer, C.; Funkhouser, G.P.; Darbe, R. A comparison study of Portland cement hydration kinetics as measured by chemical shrinkage and isothermal calorimetry. *Cem. Concr. Compos.* **2013**, *39*, 23–32. [CrossRef]

35.   Thomas, J.J.; Biernacki, J.J.; Bullard, J.W.; Bishnoi, S.; Dolado, J.S.; Scherer, G.W.; Luttge, A. Modeling and simulation of cement hydration kinetics and microstructure development. *Cem. Concr. Res.* **2011**, *41*, 1257–1278. [CrossRef]

36.   Snelson, D.G.; Wild, S.; O'Farrell, M. Heat of hydration of Portland Cement–Metakaolin–Fly ash (PC–MK–PFA) blends. *Cem. Concr. Res.* **2008**, *38*, 832–884. [CrossRef]

Publisher's Note: MDPI stays neutral with regard to jurisdictional claims in published maps and institutional affiliations.